

## BRIEF REPORTS

*Brief Reports are short papers which report on completed research or are addenda to papers previously published in the Physical Review. A Brief Report may be no longer than four printed pages and must be accompanied by an abstract.*

Time scale of quasifission from giant dipole resonance  $\gamma$ -ray yield

J. Nestler, B. B. Back,\* K. S. Drese, D. J. Hofman, S. Schadmand, R. Varma, and P. Paul  
*Department of Physics, State University of New York at Stony Brook, Stony Brook, New York 11794*  
 (Received 20 September 1994)

Giant dipole resonance (GDR)  $\gamma$  rays were measured in coincidence with reaction fragments in  $^{58}\text{Ni} + ^{165}\text{Ho}$  at 368 MeV where deep inelastic scattering and quasifission dominate the reaction. The  $\gamma$  spectrum associated with deep inelastic scattering events is well fitted by statistical cooling of projectile and target-like fragments with close to equal initial energy sharing. The  $\gamma$  spectrum associated with quasifission events is well described by statistical emission from the fission fragments alone, with only weak evidence for GDR emission from the mononucleus. A  $1\sigma$  limit of  $\tau \leq 11 \times 10^{-21}$  s is obtained for the mononucleus lifetime which is consistent with the lifetimes obtained from quasifission fragment angular distributions.

PACS number(s): 25.70.Lm, 25.70.Ji, 24.30.Cz, 24.60.Dr

The emission rate of giant dipole resonance (GDR)  $\gamma$  rays has been shown to be a useful tool for establishing the time scale of fission from a hot compound nucleus [1]. These  $\gamma$  rays can be emitted by the nucleus before it passes over the fission saddle, and then during its descent from the saddle to the scission point. In a very heavy nucleus, such as Cf, the excitation energy of the system between saddle and scission is so large that these  $\gamma$  rays dominate over those from inside the saddle. This fact was recently used to determine the time scale  $\tau_{\text{SS}}$  of the saddle-to-scission motion [2]. With  $\tau_{\text{SS}} = 30 \times 10^{-21}$  s the saddle-to-scission motion appears highly damped and rather slow.

This raises the question about the time scale of the quasifission process and whether it could also be determined from the emission of GDR-like  $\gamma$  rays. Some speculation that this was possible has already been made [1,3]. In the quasifission process the nucleus is trapped behind the (outer) conditional saddle, at a deformation close to that of a hyperdeformed nucleus, while mass equilibration takes place. During its lifetime and its evolution toward scission it could emit GDR-like  $\gamma$  rays similar to those emitted during regular fission motion outside of the regular saddle. The lifetime of the quasifission process has previously been obtained in some cases quite directly from the fission angular distribution [4], yielding  $\tau_{\text{QF}} \sim 5 - 15 \times 10^{-21}$  s for the large mass transfer considered here. This is significantly shorter than  $\tau_{\text{SS}}$ , which seems surprising at first sight. The present experiment aims at reconciling these two times.

The experiment measured the energy spectrum of high-energy  $\gamma$  rays in coincidence with primarily fission frag-

ments in a reaction that is known to proceed predominantly by quasifission, i.e., through the mononucleus, rather than by complete fusion and through the compound nucleus. The reaction studied was  $^{58}\text{Ni} + ^{165}\text{Ho} \rightarrow ^{223}\text{Am}$ , using a 368 MeV Ni beam from the Stony Brook linac. At this bombarding energy a modified extra-push model [4] predicts that the quasifission process is 73% of the capture cross section. Pertinent reaction dynamics parameters are collected in Table I.

The experimental setup and procedures follow those described in Ref. [3]. A self-supported Ho target of 520  $\mu\text{g}/\text{cm}^2$  was positioned perpendicular to the beam in a reaction chamber between four position sensitive parallel-plate avalanche counter chambers which detected reaction fragments in kinematic coincidence. High-energy  $\gamma$  rays in coincidence with the reaction fragments were detected in a large  $25.4 \times 38.1 \text{ cm}^2$  cylindrical NaI crystal with plastic anticoincidence shielding. The NaI electronics, detector calibration procedures, and pileup elimination are described in an earlier work [5].

The kinetic energies and masses of coincident reaction fragments were determined from the time of flight (timed against the linac beam burst) and the flight directions assuming two-body kinematics (see Ref. [3]). A two-dimensional plot of the kinetic energy vs mass and the projection on the mass axis are given in Fig. 1. They show the projectilelike and targetlike fragments from deep inelastic scattering and, in between, the fragments from quasifission. We note that deep inelastic scattering accounts for most of the cross section over the acceptance region from  $\theta \sim 28^\circ$  to  $83^\circ$  of the detectors, since this includes a grazing angle of  $\theta_{\text{gr}} \sim 53^\circ$  where this process is concentrated.

We consider first the  $\gamma$  spectrum in coincidence with deep inelastic events which is shown in Fig. 2(a). It is a composite of  $\gamma$  rays emitted by the projectilelike fragments (PLF's) and the targetlike fragments (TLF's) dur-

\*On leave from Argonne National Laboratory, Argonne, IL 60439.

TABLE I. Summary of reaction data for  $^{58}\text{Ni} + ^{165}\text{Ho}$  at  $E_{\text{lab}} = 368$  MeV, predicted by the modified extra-extra-push fusion model.

Energies (MeV)	Cross sections (mb)	$\langle L \rangle$ ( $\hbar$ )
$E_{\text{c.m.}} = 272$	$\sigma_{\text{reac}} = 1384$	
$Q(^{58}\text{Ni} + ^{165}\text{Ho}) = -165$	$\sigma_{\text{touch}} = 1031$	92
$Q(^{223}\text{Am} \rightarrow ^{111}\text{Ag} + ^{112}\text{Cd}) = 219$	$\sigma_{\text{capt}} = 549$	66
$T(\text{initial}) = 1.97$	$\sigma_{\text{fus}} = 146$	35

ing the statistical cooling process. These spectra were calculated using the statistical code CASCADE with the standard level density parameter of  $a = A/8.8$ . The calculated spectra were normalized to the data over the energy range from  $E_\gamma = 5.2$  to  $7.3$  MeV. The  $\gamma$  emission is averaged over  $\pm 5$  mass units around the projectile and target nuclei. The GDR parameters used for each fragment type are listed in Table II. The spectra are rather sensitive to the energy sharing between PLF's and TLF's. Fortunately, this energy sharing has recently been investigated in detail for the very similar reaction  $^{56}\text{Fe} + ^{165}\text{Ho}$  at 403 MeV by Pade *et al.* [6]. Their data are consistent with equal energy sharing or with an excitation energy sharing  $E_{\text{PLF}}^*/E_{\text{tot}}^* \approx 0.4$  as predicted by the nuclear exchange model for the damping process during the early stages of the equilibration process. The curves in Fig. 2(a) show the separate contributions due to  $\gamma$  emission from PLF's and TLF's and the sum spectrum computed for an energy sharing of  $E_{\text{PLF}}^*/E_{\text{tot}}^* = 0.45$  which pro-

duced the best overall fit to the experimental  $\gamma$  spectrum. The total excitation energy was taken as  $E_{\text{tot}}^* = 80$  MeV, which amounts to about 2/3 of the maximum possible value, i.e., that available to those fragments which emerge with fission-fragment kinetic energies. Clearly the spec-

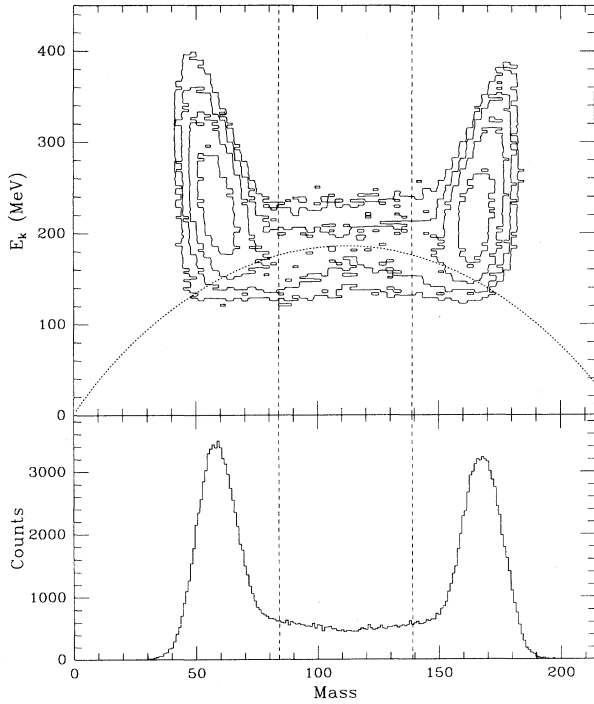


FIG. 1. Kinetic energy versus mass plot obtained in the reaction  $^{58}\text{Ni} + ^{165}\text{Ho}$  at 368 MeV. The dotted curve represents the kinetic energy expected according to the Viola systematics [10]. The bottom panel shows the projection onto the mass axis. The limits indicate the region selected for quasifission events.

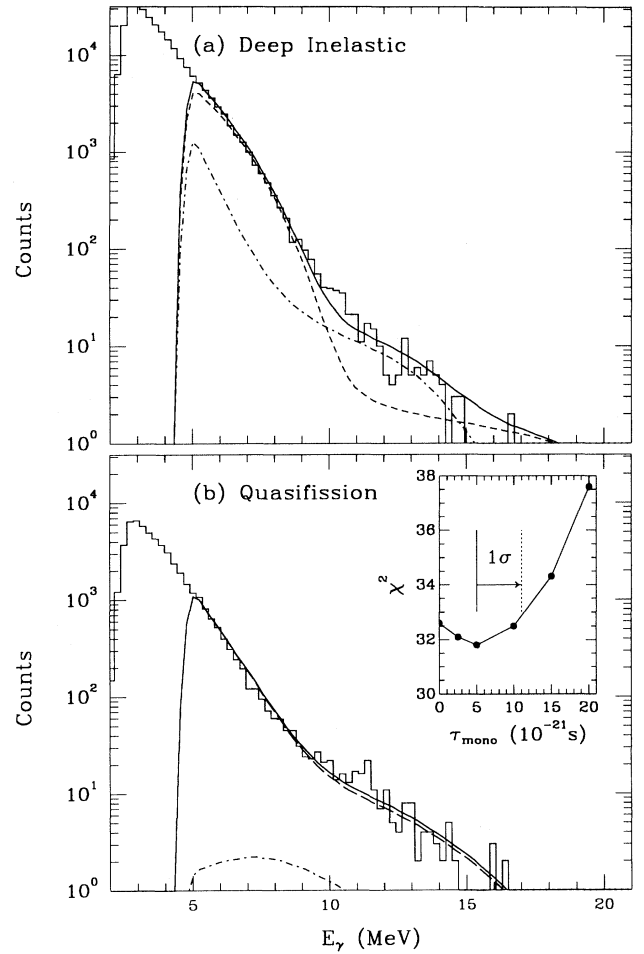


FIG. 2. (a) Top: experimental  $\gamma$ -ray energy spectrum (histogram) observed in coincidence with deep inelastic scattering events. The curves are fits assuming statistical emission of GDR  $\gamma$  rays from the PLF's (dashed line) and TLF's (dot-dashed line) and their sum (solid curve) assuming almost equal energy sharing (see text). (b) Bottom: experimental  $\gamma$ -ray spectrum (histogram) observed in coincidence with quasifission events. The curves are fits assuming statistical emission from the fission fragments only (dashed line) and the sum (solid line) including  $\gamma$  emission from the intermediate system (dot-dashed line) calculated for  $\tau_{\text{mono}} = 5 \times 10^{-21}$  s. The  $\chi^2$  dependence on  $\tau_{\text{mono}}$  is illustrated in the inset.

TABLE II. GDR parameters used to calculate  $\gamma$ -ray emission from deep inelastic scattering and quasifission. All fragments are assumed to be spherical; the mononucleus has a deformation  $\beta = 0.6$ .

Reaction product	$E(\text{GDR})$ (MeV)	$\Gamma(\text{GDR})$ (MeV)
PLF, "Ni"	20.4	6.0
TLF, "Ho"	14.4	6.0
QF, "Am"	16.4	9.3
Mononucleus	8.9, 14.6	6.3, 8.7

trum is well explained by regular statistical cooling with a sharing consistent with the results of Ref. [6]. This agrees with the fact that deep inelastic scattering proceeds on a time scale  $\tau_{\text{dis}} \sim 10^{-21}$  s, which is too fast for a measurable emission of GDR  $\gamma$  rays during the sticking time.

Next we consider the  $\gamma$  spectrum in coincidence with quasifission fragments given in Fig. 2(b). The  $\gamma$  spectrum shows the typical GDR-like behavior above 9 MeV. A statistical model fit (normalized to the data from 5.2 to 7.3 MeV) using the code CASCADE expanded to include fission [5] is able to reproduce the observed  $\gamma$  spectrum essentially without invoking any GDR  $\gamma$  rays from the combined system ("<sup>223</sup>Am").

In order to investigate the sensitivity to the time scale for the mononucleus, we then performed calculations which include the emission of  $\gamma$  rays during this stage of the reaction. The excitation energy of the system in this phase is taken as the average between the excitation energy at the saddle and scission configurations, given by  $E_{\text{saddle}}^* = E_{\text{c.m.}} + Q_{\text{cn}} - B_f$  and  $E_{\text{scis}}^* = E_{\text{c.m.}} + Q_f - E_k$ . Here,  $E_{\text{c.m.}}$ ,  $Q_{\text{cn}}$ ,  $Q_f$ ,  $B_f$ , and  $E_k$  are the center of mass energy, the fusion  $Q$  value, the fusion-fission  $Q$  value, the fission barrier, and the total fission kinetic energy, respectively. This can be considered a good approximation because the temperatures at the saddle and the scission points are not very different. The calculations were averaged over the observed (flat) mass distribution with a width of 56 mass units. The mass dependence of  $E_{\text{scis}}^*$  was included in the calculations.

The fit of the  $\gamma$  spectrum in Fig. 2(b) shows the small contribution of mononuclear  $\gamma$  rays which is needed to produce the best fit  $\chi^2$  fit ( $\chi^2/N = 1.03$  over the region  $8 \text{ MeV} < E_\gamma < 15 \text{ MeV}$ ). This yield corresponds to a mononucleus lifetimes of  $\tau_{\text{mono}} = 5 \times 10^{-21}$  s. The inset in Fig. 2(b) indicates the change of  $\chi^2$  as a function of  $\tau_{\text{mono}}$ . Following standard statistical procedures the  $1\sigma$  confidence limit that the true value falls within the fit is given by the parameter set corresponding to a fit with  $\chi_{\text{min}}^2 + 1$ . This  $1\sigma$  limit corresponds to  $\tau_{\text{mono}} < 11 \times 10^{-21}$  s. This short lifetime is in agreement with the time  $\tau_{\text{QF}} = 5 - 8 \times 10^{-21}$  s (for large mass transfer) deduced from the quasifission angular distribution in the reaction <sup>238</sup>U + <sup>64</sup>Ni [7].

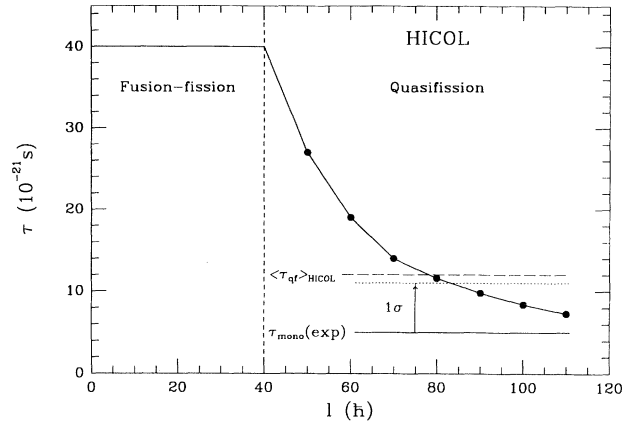


FIG. 3. Lifetimes for fission and quasifission in <sup>58</sup>Ni + <sup>165</sup>Ho as a function of the  $L$  value as predicted for full one-body dissipation. The lifetimes for quasifission ( $L \geq 40$ ) are computed with the code HICOL; the saddle-to-scission times for CN fission ( $L < 40$ ) are from Ref. [9].

Finally, these limits can be compared to the reaction times  $\tau_{\text{QF}}$ , for quasifission predicted by the HICOL reaction dynamics code of Feldmeier [8] which includes full one-body dissipation and assumes that the one-body dissipation smoothly changes from the window formula for necked-in shapes to the wall formula for more compact shapes. Figure 3 gives the quasifission reaction times as a function of  $L$  computed with HICOL for the present reaction and bombarding energy. Quasifission sets in at an angular momentum threshold  $L \geq 40$ , and one obtains an  $L$ -weighted lifetime  $[\sum \sigma(L)\tau(L) / \sum \sigma(L)]$  with limits  $L=40-110$  of  $\langle \tau_{\text{qf}} \rangle = 12 \times 10^{-21}$  s as indicated by the dashed line in Fig. 3. This is somewhat longer than our upper limit (dotted line in Fig. 3), in agreement with an earlier finding that HICOL overpredicts reaction times by about a factor of 2 [8]. We also indicate in Fig. 3 the predicted saddle-to-scission time [9] for compound nuclear (CN) fission which prevails for  $L < 40$ . It is in essential agreement with the saddle-to-scission time  $\tau_{\text{SS}} = 30 \times 10^{-21}$  s found from  $\gamma$ -ray emission in CN fission of hot Cf [2]. The shorter quasifission times are mainly due to the fact that this process is concentrated at higher  $L$  values.

In summary, the present experiment demonstrates that in both deep inelastic and quasifission reactions, very few GDR  $\gamma$  rays are seen from any intermediate system, in agreement with the short reaction lifetimes obtained by other experimental techniques.

This work was supported in part by the U.S. National Science Foundation and by the U.S. Department of Energy, Nuclear Physics Division under Contract No. DE-FGO293ER40780. J.N. and K.D. acknowledge support by fellowships from the Friedrich-Ebert-Stiftung and the Deutsche Akademischer Austauschdienst, respectively.

- [1] R. Butsch, D. J. Hofman, C. P. Montoya, P. Paul, and M. Thoennessen, *Phys. Rev. C* **44**, 1515 (1991).
- [2] D. J. Hofman, B. B. Back, I. Diószegi, C. P. Montoya, S. Schadmand, R. Varma, and P. Paul, *Phys. Rev. Lett.* **72**, 470 (1994).
- [3] I. Diószegi, D. J. Hofman, C. P. Montoya, S. Schadmand, and P. Paul, *Phys. Rev. C* **46**, 627 (1992).
- [4] W. Q. Shen, J. Albinski, A. Gobbi, S. Gralla, K. D. Hildenbrand, N. Herrmann, J. Kuzminski, W. F. J. Müller, H. Stelzer, J. Töke, B. B. Back, S. Bjørnholm, and S. P. Sørensen, *Phys. Rev. C* **36**, 115 (1987).
- [5] R. Butsch, M. Thoennessen, D. R. Chakrabarty, M. G. Herman, and P. Paul, *Phys. Rev. C* **41**, 1530 (1990).
- [6] D. Pade, W. U. Schröder, J. Töke, J. L. Wile, and R. T. DeSouza, *Phys. Rev. C* **43**, 1288 (1991).
- [7] J. Töke, G. X. Dai, S. Gralla, A. Gobbi, K. D. Hildenbrand, W. F. J. Muller, A. Olmi, H. Stelzer, B. B. Back, and S. Bjørnholm, *Nucl. Phys.* **A440**, 327 (1985).
- [8] H. Feldmeier, *Rep. Prog. Phys.* **50**, 915 (1987).
- [9] N. Carjan, A. J. Sierk, and J. R. Nix, *Nucl. Phys.* **A452**, 381 (1986).
- [10] V. E. Viola, K. Kwiatkowski, and M. Walker, *Phys. Rev. C* **31**, 1550 (1985).